Acta Oncologica Vol. 32, Nos. 7/8, pp. 869–872, 1993

BETA CAMERA LOW ACTIVITY TUMOR IMAGING

KAJ LJUNGGREN, SVEN-ERIK STRAND, CRISTER P. CEBERG, HANS SJÖHOLM, DAN ELMQVIST, ARNE BRUN and LEIF G. SALFORD

A new technique, the beta camera, to complement film autoradiography, with fast quantitative imaging of beta particle-emitting radionuclides has been developed. It consists of a thin plastic scintillator and a light-sensitive microchannel plate detector. The thin tissue sample is mounted on the scintillator. Our first system had a high background and a moderate spatial resolution of 900 μm. We now report an improved system with a photomultiplier tube mounted on the scintillator of the microchannel plate detector. Only events registered by both detectors are accepted. A fast coincidence unit processes the signals, and if a time overlap exists, an event is generated in the beta camera. In the coincidence mode, images with low activity distribution of ^{201}Tl (count rate 1 s^{-1}) in 50 μm-thick slices of a human glioma tumor could be recorded with a spatial resolution of 500 μm.

In systemic radiation therapy (e.g., radioimmunotherapy) and in diagnostic nuclear medicine, knowledge of the activity distribution within a tissue at the submillimeter level is essential to correctly estimate the localized absorbed dose and the absorbed dose distribution. In vivo techniques, i.e., pinhole-planar or pinhole-SPECT imaging can be achieved with a resolution in the order of 1–3 mm (1, 2). In experimental studies in animals or on biopsy specimens from patients, more detailed information on the spatial distribution of a radiotracer is often desired. Today, film autoradiography is used either as whole-body or organ autoradiography, or as the more detailed microscopical or electron microscopy autoradiography (2), with resolutions ranging from tenths of a mm to a few μm. Some of the drawbacks of these techniques are their low sensitivity, time-consuming preparation, and the long exposure time (days-months). Faster techniques are needed, especially when imaging short-lived radionuclides, or when an overview of the activity distribution is desired. Quantification of film autoradiograms is cumbersome, and digitalization is needed, especially when the data are to be used to quantify activity uptake and absorbed dose.

The film autoradiography technique has been used for decades. The technique with whole body autoradiography was invented by Ullberg (3) and has since then been used in many applications. At our laboratory we have used this technique to study ^{111}In distributions in animals (4, 5).

A faster alternative technique that allows direct quantification has been invented by us, the beta camera. The apparatus easily performs fast, quantitative imaging of beta particles, or all charged particle emitting radionuclides, e.g., β- and α-emitting radionuclides. The system is reported in detail elsewhere (6–10). Our earlier beta camera systems could measure activities in the order of 100 Bq with a spatial resolution of about 900 μm. A newly implemented innovation using the coincidence technique and a new detector system has improved the detectability down to a few Bq and enhanced spatial the resolution to about 500 μm.

The aim of this paper is to describe the potential of low activity beta camera imaging. We thus report the first clinical study of activity distributions in human tumors (^{201}Tl in human glioma tumors) with the new beta camera system. Because of very low signal-to-noise ratio, activity

Received 1 February 1993.
Accepted 8 June 1993.
From the Departments of Radiation Physics (K. Ljunggren, S.-E. Strand, C. P. Ceberg), Clinical Neurophysiology (H. Sjöholm, D. Elmqvist), Neuropathology (A. Brun) and Neurosurgery (L. G. Salford), Lund University Hospital, Lund, Sweden.
Correspondence to: Dr Kaj Ljunggren, Radiation Physics Department, Lund University Hospital, S-221 85 Lund, Sweden.
Presented at the 3rd Scandinavian Symposium on Monoclonal Antibodies in Diagnosis and Therapy of Cancer, October 30–31, 1992, Helsinki, Finland.

was too low to be detected with the old beta camera system. However, with our new technique good quality images were acquired within a day.

Material and Methods

Beta camera system. Details of the beta camera are given elsewhere (6-10). Briefly, it consists of a thin plastic scintillator (NE 102A, 0.01–0.9 mm thick) and a light sensitive microchannel plate detector (MCP, ITL Ltd, England). The tissue sample (10–50 μm thick) is mounted on the scintillator with a plastic film (Mylar, 3 μm thick) between the sample and the scintillator (Fig. 1). When a beta particle interacts with the scintillator, the MCP collects the scintillation light, and the position is calculated from the electron avalanche impinging on the resistive anode. The whole detector system is housed in a freezer and kept at −20°C. This makes thermal noise from the system low, but more importantly makes it possible to transfer frozen sections to the detector, facilitating imaging without having to fix the tissue samples.

The new technique consists of a photo-multiplier tube mounted on the scintillator of the MCP. Only events which are registered from both scintillation light detectors are accepted. The pulses from the detectors are discriminated in separate discriminators, and logical timing signals are generated with small time windows. A fast coincidence unit processes these logical signals, and if a time overlap exists a new pulse is generated and used as a gate signal for the acquisition unit of the beta camera system.

Radionuclides. The radionuclides ^{14}C and ^{201}Tl were studied. The former in a test strip phantom (Autoradiographic [^{14}C] micro-scales RPA.504L, Amersham) and ^{201}Tl as thallium chloride administered to glioma patients. The decay properties for ^{14}C (average beta energy 49.5 keV, $T_{1/2}$ 5730 y) and ^{201}Tl (photons 135.3–167.4 keV, X-rays 11.0–80.1 keV, conversion electrons 1.57–165.3 keV, Auger electron groups 2.7–77.3 keV, $T_{1/2}$ 73.1 h) were derived from Weber et al. (11).

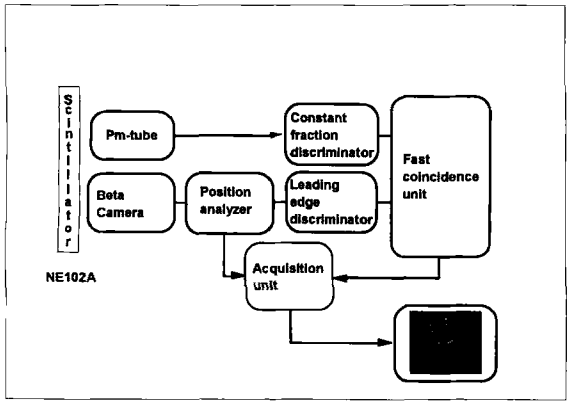

Fig. 1. Block scheme for the coincidence unit.

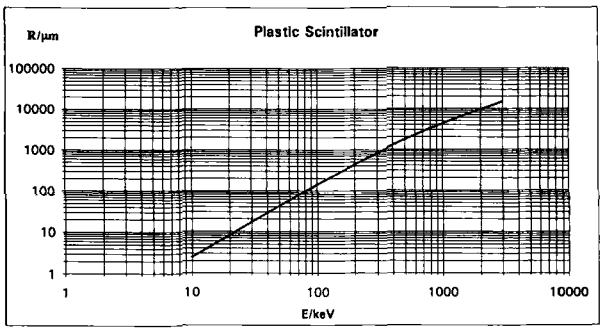

Fig. 2. Electron range in plastic scintillator versus electron energy (12).

Range of electrons. The sensitivity and resolution of the beta camera system are dependent on the range of electrons emitted in the sample. Emitted electrons are a complex mixture of different energies. In Fig. 2 the range of electrons in plastic scintillator material is plotted for different energies (12).

Phantom measurements. To measure the contrast of the system, images of a ^{14}C test strip were collected. The strip ([^{14}C] micro-scales, Amersham) is a ^{14}C-labelled polymer with a thickness of 120 μm, and is divided into 8 sections with activities of 32.7, 26.2, 19.6, 13.2, 8.7, 4.5, 2.2, 1.1 kBq/g, with a total activity of 74 Bq. Images were acquired for 12–48 h with and without the coincidence unit. The contrast was calculated form regions of interest (ROI) over the individual sections, and in the background below the strip. The contrast was calculated as

$$C = \frac{N_2/n_2}{N_1/n_1}$$

where N_2 is the number of counts (net) to the ROI in the ^{14}C test strip image with n_2 pixels, and N_1 is the number of counts in the background ROI with n_1 pixels.

Patient studies. Patients with malignant brain tumors, supratentorial gliomas (grade III–IV astrocytomas according to Kernohan), were injected intravenously with 75 MBq ^{201}Tl 4 h before surgery. Half an hour after the injection, a SPECT study was done with a Tomomatic 64 system (Medimatic, Denmark). Three hours after the injection, the neurosurgical operation started, and one hour later the tumor was resected en bloc together with a small portion of immediately adjacent brain tissue. The tumor specimen was immediately divided longitudinally and both halves were glued to cork plates, with the cut surface away from the plate. The first slices from the two cork plates were similar, and were used to compare ^{201}Tl distribution with histological findings. Immediately after the specimens had been glued to the cork plates, they were frozen in isopenthane, containing dry ice, within 30 s after resection. The specimen on one of the cork plates was freeze-sectioned at −20°C into 10, 25, or 50 μm-thick slices, which were picked up on objective glasses made of perspex and

transferred frozen to the beta camera. Six hours after resection, these slices were mounted on the beta camera, where they were imaged for 12 h. The specimen on the second cork plate was used for histopathologic examination, the findings of which were compared with the beta camera image to identify areas of malignant and normal tissue.

Results

Phantom studies The noise level (i.e., the background count rate) was lowered from 50 cps to 0 cps when the coincidence unit was used. In ^{14}C test strip images (Fig. 3) the background decreased substantially, and the strip segment contrast increased. The Table shows that with the coincidence unit, contrast improved 10- to 50-fold. Even the lowest activity was visible in the coincidence image. The sensitivity of the system was calculated by dividing the number of counts in the image, corrected for background, by the activity in the strip. Sensitivity was $10^{-2}\ s^{-1}\ kBq^{-1}\ g$ without and $10^{-3}\ s^{-1}\ kBq^{-1}\ g$ with the coincidence unit.

Patient studies. In the coincidence mode, images of the low activity distribution of ^{201}Tl in 50 μm-thick slices of human glioma tumor were obtained (Fig. 4). The count rate during acquisition from the samples was in the order of 1 s^{-1} in the whole image. Histological examination of the imaged sections revealed that tumoral and normal

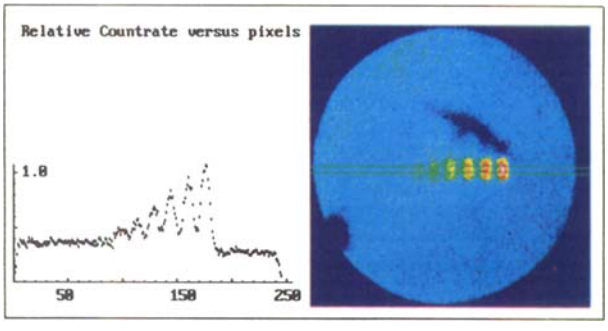

a)

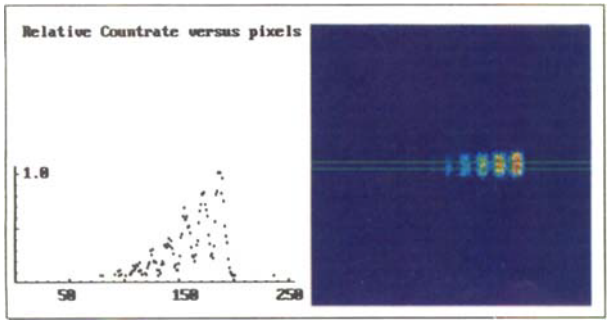

b)

Fig. 3. Image and count rate profile of ^{14}C test strip. a) Old beta camera system with conventional technique. Note the high background level. b) New system beta camera with coincidence technique. Note the much better singal/noise ratio, and that all eight strips are detectable.

Table 1

Contrast in images from ^{14}C test strips

Test strip		Contrast	
Activity conc. (kBq/g)	Activity (Bq)	Without coincidence unit	With coincidence unit
32.7	22.4	1.4	14.1
26.2	17.9	1.2	12.1
19.6	13.4	1.0	9.4
13.2	9.0	0.7	6.4
8.7	6.0	0.3	5.1
4.5	3.1	0.2	4.4
2.2	1.5	<0.1	3.0
1.1	0.75	<0.1	<0.1

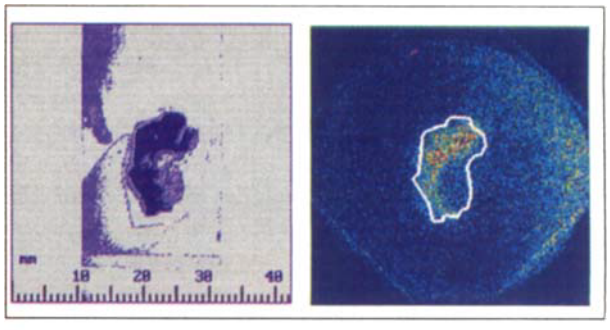

a) b)

Fig. 4. Tumor resected from a patient with glioma. The patient received an injection with 75 MBq ^{201}Tl 4 h prior to operation. a) Histological section showing tumor (darker areas) and normal brain tissue. b) Beta camera image showing activity distribution corresponding to the tumor areas identified in A). The white contour obtained in the histological image is superimposed on the beta camera image.

brain tissue (Fig. 4a), corresponded well with the beta camera images (Fig. 4b) whereas areas with tumor tissue showed ^{201}Tl uptake, whereas areas with normal or mainly normal brain tissue lacked ^{201}Tl uptake.

Discussion and Conclusion

We report the first successful imaging with an improved beta camera of ^{201}Tl in tumor samples from patients with glioma. The coincidence technique considerably increased the signal/noise ratio, and it was possible to image very low activities.

The new system showed a substantial contrast enhancement, and background level was reduced to almost zero. Thus, low activity measurements with activities in the range of Bq is feasible with this new system.

Although the sensitivity is low in this system, it is still higher than that of ordinary autoradiography film techniques. In a study of ^{14}C-labelling in a rat, a beta camera image was obtained within 6 h compared to 52 days with film autoradiography (7). Another advantage is that no

prior knowledge of the actual activity in the sample is necessary to avoid over- or underexposure. The image is acquired on line, that is, acquisition can be followed and terminated when the desired information is obtained. Thus the image information is available immediately after the acquisition in contrast to film techniques in which processing, calibration, and digitalization must be done. In systemic radiation therapy (radioimmunotherapy), the absorbed dose distribution in the patient must be determined (13–15). But to evaluate the biological effect and relate it to cell killing, the microscopical distribution of the absorbed dose is essential (16). A combination of both macroscopical and microscopical information is necessary for the complete evaluation of dosimetry with all kinds of radiopharmaceuticals (17).

In conclusion, we have improved the beta camera for low activity imaging in the order of a few bequerels, and obtained successful imaging of ^{201}Tl in human brain tumors. We believe that the beta camera will be an important instrument for future studies of activity distributions, and are now developing a three-dimensional technique for both the activity distribution and the absorbed dose distribution in the tissue.

ACKNOWLEDGEMENTS

The authors wish to express their thanks to the Swedish Natural Science Research Council (grant No. F-FU 1621-111), Swedish Association for Technical Support (grant No. 89-0247P), Kamprad Foundation for Cancer Research, Lund, Nilsson Foundation for the Treatment of Cancer, The Faculty of Medicine, Lund University, and Lund University Hospital. Thanks are also due to Ms Catharina Blennow and Ms Kerstin Sturesson for valuable technical assistance, and to Anders Sandell for fruitful discussions.

REFERENCES

1. Widner H, Jönsson B-A, Hallstadius L, Wingårdh K, Strand S-E, Johansson B. Scintigraphic method to quantify the passage from brain parenchyma to the deep cervical lymph nodes in rats. Eur J Nucl Med 1987; 13: 456–61.
2. Rogers AW. Techniques of autoradiography. Amsterdam: Elsevier/North-Holland Biomedical Press, 1979.
3. Ullberg S, Larsson B, Tjävle H. Autoradiography. In: Glenn HJ, Colombetti LG, eds. Biologic applications of radiotracers. Boca Raton, FL: CRC Press Inc., 1982: 55–108.
4. Jönsson B-A, Strand S-E, Larsson BS. A quantitative autoradiographic study of the heterogenous activity distribution of different indium-111-labeled radiopharmaceuticals in rat tissues. J Nucl Med, 1992; 33: 1825–33.
5. Jönsson B-A, Strand S-E, Emanuelsson H, Larsson B. Tissue, cellular, and subcellular distribution of indium radionuclides in the rat. In: Howell RW, Narra VR, Sastry KSR, Rao DV, eds. Biophysical Aspects of Auger Process. New York: American Institute of Physics, 1992: 249–72.
6. Ljunggren K, Strand S-E. Development of a digital imaging detector based on microchannel plates for biomedical samples emitting uncharged and charged particles. Nucl Instr Meth 1988; A273: 784–86.
7. Ljunggren K, Strand S-E. Beta camera for static and dynamic imaging of charged particle emitting radionuclides in biologic samples. J Nucl Med 1990; 31: 2058–63.
8. Ljunggren K, Strand S-E. An improved imaging detector for charged particle emitting radionuclides. In: Höfer R, Bergmann H, Sinzinger H, eds. Radioactive isotopes in clinical medicine and research. Stuttgart: Schattauer, 1991: 267–73.
9. Ljunggren K, Strand S-E. Imaging detector for static and dynamic studies in biological samples. Nucl Instr Meth 1991; A310: 475–8.
10. Strand S-E, Ljunggren K, Kairemo K, et al. Functional imaging and dosimetric applications of the beta camera in radioimmunodiagnosis and radioimmunotherapy. Antibody Immunoconjug Radiopharm 1991; 4: 631–5.
11. Weber DA, Eckelman KF, Dillman LT, Ryman JC. MIRD: Radionuclide data and decay schemes, Society of Nuclear Medicine, 1989.
12. International Commission on Radiation Units and Measurements, ICRU Report No. 37, 'Stopping powers for electrons and positrons'. ICRU, Bethesda, MD, 1984.
13. Ljungberg M, Strand S-E. Quantitative SPECT in oncological nuclear medicine. Application in dose planning for radionuclide therapy. Hospimedica 1988; 6: 17–21.
14. Ljungberg M, Strand S-E. Dose planning with SPECT. Int J Cancer, 1988, (Suppl. 2): 67–70.
15. Strand S-E, Ljungberg M. Absorbed dose planning in radionuclide therapy based on quantitative SPECT. Antibody Immunoconjug Radiopharm 1991; 4: 673–80.
16. Hui TE, Fisher DR, Press OW, Eary JF, Weinstein JN, Badger CC. Localized beta dosimetry of ^{131}I-labeled antibodies in follicular lymphoma. Med Phys 1992; 19: 97–104.
17. Jönsson B-A, Strand S-E, Andersson L. Radiation dosimetry for indium-111-labeled anti-CEA-F(ab')$_2$ fragments evaluated from tissue distribution in rats. J Nucl Med 1992; 33: 1654–60.